ACE Deliverable *2.2D4*

Report on existing and new measurement procedures

Project Number: FP6-IST 508009
Project Title: Antenna Centre of Excellence
Document Type: Deliverable

Document Number:
Contractual date of delivery: 31st March 2005
Actual Date of Delivery: 29 March 2005
Workpackage: 2.2-2
Estimated Person Months:
Security (PP,PE,RE,CO): PP
Nature: Report
Version: 1.1
Total Number of Pages: 42
File name: 2.2.D4.pdf
Editors: J. Carlsson (CHALMERS), A.K. Skrivervik (EPFL), C. Icheln (HUT)
Participants: J. Carlsson (CHALMERS), P.S. Kildal (CHALMERS), Marta Martínez Vázquez (IMST), A.K. Skrivervik (EPFL), C. Icheln (HUT), A. Moreira (IST), L. Duchesne (Satimo), A. Johansson (LU), P.R. Rogers (UoB)

Abstract

The present document is a review of existing and new measurement procedures for small terminal antennas.

Keyword List

Terminal antenna measurement procedures, Radiation efficiency, Mean effective gain, Mean effective directivity, Diversity gain, Total radiated power, Total isotropic sensitivity

Contents

Contents 2

1 Introduction 3

2 Summary 4

3 Definition of measurement quantities for small passive terminal antennas 5
3.1 Radiation pattern 5
3.2 Radiation efficiency and total radiation efficiency 5
3.3 Mean effective gain – MEG 6
3.4 Mean effective directivity – MED 6
3.5 Diversity gain 6

4 Definition of measurement quantities for small active terminals 7
4.1 Total radiated power – TRP 7
4.2 Near-Horizon partial radiated power – NHPRP 7
4.3 Elevation weighted radiated power 7
4.4 Implemented diversity gain 7
4.5 Total isotropic receiver sensitivity – TIS 8
4.6 Near-Horizon partial isotropic sensitivity - NHPIS 8
4.7 Elevation weighted receiver sensitivity 8
4.8 Average fading sensitivity 8
4.9 Channel capacity 8

5 Measurement methods 10
5.1 Anechoic chamber 10
5.1.1 3D Measurements 11
5.1.2 Spherical Near Field Antenna Measurements 14
5.1.3 STARGATE and STARLAB spherical near field measurement systems 15
5.1.4 Spherical Angular Sampling Criteria 17
5.1.5 Definition of the maximum radius for the AUT 19
5.1.6 Example of passive measurements of omni-directionnal antennas 20
5.1.7 Configuration of active measurements 21
5.1.8 Example of active measurement results 23
5.1.9 Human body interaction 24
5.1.10 Alternative 3-D field measurement system 25
5.1.11 Radio-Channel sounder measurements 26
5.2 Reverberation chamber 27
5.3 Wheeler Cap Method 32
5.4 Measurement of electrically very small antennas 34
5.4.1 The “random” positioner 35
5.4.2 Example of measurement 36

6 References 39

The information contained in this document should be used only for the scope of the contract for which this document is prepared.

1 Introduction

The trend towards miniaturization of communication equipment is not only limited to electronic circuits or batteries, but concerns more and more the antennas used in such equipment. The design of these electrically small antennas is not an easy task, and mainly consists of making compromises between dimensions, bandwidth, efficiency and gain. Once a miniature antenna has been designed, the next difficulty is to characterize it.

Electrically small antennas are difficult to measure properly because, due to the limited size of ground planes or feeding baluns, they are neither purely symmetrical nor anti-symmetrical. Therefore, when such an antenna is connected to a measuring device, a current will flow in the outer conductor of the cable connecting the antenna, creating spurious radiation. In fact, this spurious radiation can be so important that it will frequently mask completely the characteristics of the antenna under test and will cause overestimation of the gain up to 10 dB or more. Impedance measurements are also affected, as the measurement will yield the impedance of the antenna formed by the small antenna plus the connecting cable. Furthermore, when a small antenna is mounted on a casing, the latter will participate to the radiation, and its effect should be taken into account when characterizing a mobile communication device. To complicate the problem, the polarization is seldom well defined. Thus, the only way to obtain useful information about the antenna behaviour of a mobile communication device is to test it under operating condition, and the relevant features will be its gain and efficiency.

The information contained in this document should be used only for the scope of the contract for which this document is prepared.

2 Summary

The table below shows the mapping of measurement methods on quantities relevant for small terminal antennas. The different quantities as well as the measurement methods are described in the following.

	Measurement method				
Quantity	Anechoic chamber	Near-field scanning	Reverberation chamber	Wheeler cap	Very small antenna method
3D-pattern	X	X			
Radiation efficiency	X	X	X	X	X
MEG – Mean Effective Gain	X	X			X
MED – Mean Effective Directivity	X	X			
Diversity gain	X	X	X		
TRP – Total Radiated Power	X	X	X		X
Weighted radiated power	X	X			
Implemented diversity gain			X		
TIS – Total Isotropic Sensitivity	X	X	X		X
Weighted receiver sensitivity	X	X			
Average fading sensitivity			X		
Channel capacity			X		

Table 1. Mapping of measurement methods on quantities.

The information contained in this document should be used only for the scope of the contract for which this document is prepared.

3 Definition of measurement quantities for small passive terminal antennas

3.1 Radiation pattern

The far-field pattern is measured on the surface of a sphere with constant radius around the antenna under test (AUT). Each location on the sphere is identified by the standard directional angles ϕ and θ of the spherical coordinate system. Usually, radiation patterns of antennas are 3-dimensional, though they are often displayed as 2-D cuts in the principal planes (usually E and H planes). They can be given as amplitude patterns defined by the vector sum of the two orthogonally polarized radiated field components. Often, also the additional phase pattern is needed, i.e. to obtain the complex-valued 3-D pattern, which is especially relevant when evaluating the diversity performance of multi-element mobile terminals.

The following quantities of interest can be derived from the 3D measured radiation pattern:

- Gain
- Directivity
- Side lobe level
- 3 dB beam-width
- Position of nulls
- Axial ratio
- Cross-polarization levels
- Front-to-back ratio
- etc.

3.2 Radiation efficiency and total radiation efficiency

The *radiation efficiency* is defined as the ratio of the radiated power to the net power delivered to the antenna. The *total radiation efficiency* is defined as the ratio of the radiated power to the maximum available power from a 50 Ω source. Thus, this includes losses in the antenna itself, losses in the near-in environment of the antenna, and impedance mismatch.

The definitions are given by the following formulas,

$$\begin{cases} Radiation\ Efficiency = \dfrac{P_{rad}}{P_{in}} \\ Total\ \ Radiation\ Efficiency = \dfrac{P_{rad}}{P_{\max}} = \left(1 - \left|S_{11}\right|^2\right)\dfrac{P_{rad}}{P_{in}} \end{cases}$$

The information contained in this document should be used only for the scope of the contract for which this document is prepared.

3.3 Mean effective gain – MEG

The *Mean Effective Gain* (MEG) is the ratio of the actually received mean power by the antenna under test to the mean power received from two hypothetical isotropic antennas in the same environment and matched to the θ- and φ-polarizations, respectively. As detailed in [1], the MEG may be obtained using a surface integration,

$$\Gamma(f) = \frac{\oint \left(G_\theta(\Omega; f) Q_\theta(\Omega; f) + G_\varphi(\Omega; f) Q_\varphi(\Omega; f) \right) d\Omega}{\oint \left(Q_\theta(\Omega; f) + Q_\varphi(\Omega; f) \right) d\Omega}$$

where $G_{\theta,\varphi}(\Omega; f)$ is the θ, φ-polarization component of the gain pattern for the antenna under test measured at the frequency f, and Ω is the solid angle describing the direction.

3.4 Mean effective directivity – MED

The *Mean Effective Directivity* (MED) is defined as the ratio of the MEG and the radiation efficiency,

$$MED = \frac{MEG}{Radiation\ \ Efficiency}$$

3.5 Diversity gain

Diversity gain can be divided into *effective, actual* and *apparent diversity gains*. The parameters are defined at a specific cumulative probability level (CDF), e.g. 1 %, when a specified diversity algorithm is used. The environment needs also to be defined and can e.g. be assumed to be isotropic, i.e. equal probability for all angles of arrival or it can be weighted in e.g. elevation in which case a certain range of angle of arrival is more probable than others.

By *effective diversity gain* we mean the gain relative to what is obtained by using a separate single antenna with 0 dB radiation efficiency, i.e. compared to an ideal reference in free space. *Actual diversity gain* is defined as the gain relative to a single antenna placed close to a lossy object such as the user or a head phantom and *apparent diversity gain* is defined as relative the strongest branch.

The information contained in this document should be used only for the scope of the contract for which this document is prepared.

4 Definition of measurement quantities for small active terminals

4.1 Total radiated power – TRP

The *Total Radiated Power* (TRP) is a measure of the power the device actually radiates, when non-idealities such as mismatch and losses in the antenna are taken into account. The TRP is defined as the integral of the power transmitted in different directions over the entire radiation sphere,

$$P_{TRP} = \frac{1}{4\pi}\oint\left(P_{tx}G_{\theta}(\Omega; f) + P_{tx}G_{\varphi}(\Omega; f)\right)d\Omega$$

where $G_{\theta,\varphi}(\Omega; f)$ is the θ, φ-polarization component of the gain pattern for the antenna under test measured at the frequency *f*, and Ω is the solid angle describing the direction. P_{tx} is the transmit power level of the terminal so that $P_{tx}G_{\theta,\varphi}(\Omega; f)$ is the actually transmitted power-level, also known as EIRP, in the θ, φ-polarization and in the direction Ω for frequency *f*.

4.2 Near-Horizon partial radiated power – NHPRP

The Near–Horizon partial radiated power is similar to TRP but the integral of transmitted power is integrated in elevation over ± 45 degrees and ± 30 degrees near the horizon.

4.3 Elevation weighted radiated power

The elevation weighted radiated power is similar to TRP but weights are introduced in the integral of the transmitted power so that some directions are in favour over others. This is done on order to simulate a particular type of environment.

4.4 Implemented diversity gain

The implemented diversity gain is defined as the diversity gain of the active terminal when the integrated software in the device provides the diversity combination.

The information contained in this document should be used only for the scope of the contract for which this document is prepared.

4.5 Total isotropic receiver sensitivity – TIS

The *Total Isotropic Sensitivity* (TIS) is defined as,

$$TIS = \frac{4\pi}{\oint\left[\frac{1}{EIS_{\theta}(\Omega; f)} + \frac{1}{EIS_{\varphi}(\Omega; f)}\right]d\Omega}$$

where the effective isotropic sensitivity (*EIS*) is defined as the power available at the antenna output such as the sensitivity threshold is achieved for each polarization.

4.6 Near-Horizon partial isotropic sensitivity - NHPIS

The Near–Horizon partial isotropic sensitivity is similar to TIS but the integral of received sensitivity is integrated in elevation over ± 45 degrees and ± 30 degrees near the horizon.

4.7 Elevation weighted receiver sensitivity

The elevation weighted receiver sensitivity is similar to TIS but weights are introduced in the integral so that some directions are in favour over others. This is done on order to simulate a particular type of environment.

4.8 Average fading sensitivity

The total isotropic sensitivity (TIS) is equal to the sensitivity in dBm measured directly on the receiver input port, degraded by the radiation efficiency of the antenna. The TIS can be measured both in an anechoic chamber and in a reverberation chamber, but the procedure is laborious. The reverberation chamber offers in addition the possibility of a much faster measurement in an actual fading environment, with a continuously fading signal present at the terminal. This is a way of characterizing mobile terminals on reception which is very realistic compared to an actual operation of the terminal. However, this Average Fading Sensitivity (AFS) gives a larger dBm value than TIS (for the same BER or FER). The difference seems to be constant in dB, and work is in progress to theoretically evaluate this constant. At the moment it is sufficient to point out that the differences (in dBm) between the AFS of different phones seem to be the same as between the TIS of the same phones. Measured results can be found in [2].

4.9 Channel capacity

There is presently a lot of attention given to the research on future communication systems which continuously adapt to fading. A popular candidate for such is a so-called MIMO system (Multiple Input Multiple Output), where multiple ports on both the transmitting and receiving sides are used to generate several communication channels between which the

The information contained in this document should be used only for the scope of the contract for which this document is prepared.

signals are distributed in an optimum manner. MIMO antennas and terminals require special testing instrumentation. The quality of a MIMO system in a fading multipath environment is characterized by the maximum available capacity in bits/sec/Hz. Antennas for MIMO systems degrade the capacity due to both their radiation efficiency and correlation between received signals, of which the former is a dominating factor.

The information contained in this document should be used only for the scope of the contract for which this document is prepared.

5 Measurement methods

5.1 Anechoic chamber

A fully anechoic chamber (FAC) is a free-space measurement environment, i.e. all walls are completely covered by RF absorbing material, and no conducting surfaces are present. Thereby, high field homogeneity of ± 0.5 dB can be obtained over a very wide frequency range. This homogeneity is required by antenna calibration standards [3] (pp. 19-20). In excellent anechoic chambers field homogeneity as good as ± 0.1 dB can be achieved. Hereby, the measurement of the directly transmitted electromagnetic field is possible without considerable interference from reflected fields. The typical distance between the antenna under test (AUT) and the measurement antenna is 2 – 5 m. Distances between the antennas and the walls, as well as between the antennas and the floor and ceiling, are typically 1 – 3 m. Those traditional chambers were designed for rather large antennas and cause rather high costs. For the much smaller terminal antennas alternatives were sought after with considerably smaller space requirements. Therefore, one can nowadays find anechoic chambers especially for small antennas with the measurement distance reduced to 1 m, and the distance to the walls to 50 cm [4]. Furthermore, the motors and the positioners cause interferences to the radiation patterns of small antennas, and therefore multiprobe systems have been developed that avoid the problem of having to move the antenna under test (AUT) or the measurement probe around one or two axes. These multi-probe systems also decrease the measurement time drastically from often about 1 hour or more for a full 3-D pattern to one minute or less.

For small terminal antennas the total radiated power (TRP) or efficiency is usually more relevant than the 3-D radiated field patterns, since for those electrically small antennas no distinct main beam exists. The TRP can be determined by integrating the 3-D gain pattern. The radiation efficiency is obtained from the ratio of maximum gain to directivity.

In order to get the diversity gain of an antenna system it is first necessary to measure the complete (i.e. amplitude and phase) radiation pattern of each branch and then perform a post processing of the data. Included in the post processing are calculations of the correlation coefficients between the field patterns taken a propagation model into account. The propagation model can be uniform or include some weight to model a specific environment.

The information contained in this document should be used only for the scope of the contract for which this document is prepared.

5.1.1 3D Measurements

The 3-dimensional measurement set-up consists of a roll positioner with or without head model, which is installed on an azimuth positioner. The azimuth positioner performs an movement that generates a Theta (θ) turn, from –18° to 0°, whereas the roll positioner establishes a roll scan that describes Phi (ϕ), from –180° to 180°. The resulting roll over azimuth positioner allows fully 3-dimensional radiation diagrams. The minimum angle step of both axes, which determines the positioning accuracy of the system, is 0.5°. An example of the complete measurement system including positioner and head model inside the measurement chamber is shown in Figure 1. To simulate the interaction of the user with a mobile device, an artificial phantom head can be mounted on the roll positioner.

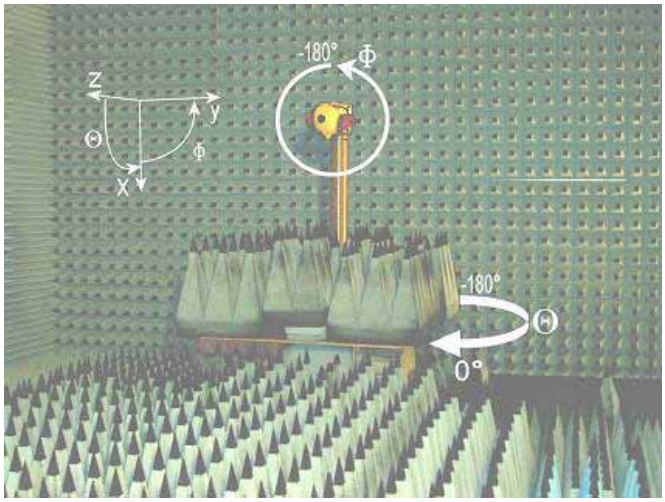

Figure 1. 3-dimensional measurement set-up at IMST. The arrows show the turning direction of azimuth and roll positioner. The drawn coordinates system is used to show the radiation direction from the device under test.

The electrical part of the system contains a base station simulator, the measurement antenna, the control antenna and the mobile station. The measurement antenna is mounted in far field distance to the mobile phone, whereas the control antenna is placed near the mobile station. Both antennas are connected to the base station simulator. During post processing, the resulting fields are calculated from the measured field components. In addition to 3D-radiation characteristics, the total radiated power (TRP) or the total isotropic sensitivity (TIS) as well as effective isotropic radiated power (EIRP) or the effective isotropic sensitivity (EIS) can be obtained. This measurement setup allows measuring both active and passive devices, and can be used to measure devices according to the most usual recommendations, such as CTIA [5], [6].

The information contained in this document should be used only for the scope of the contract for which this document is prepared.

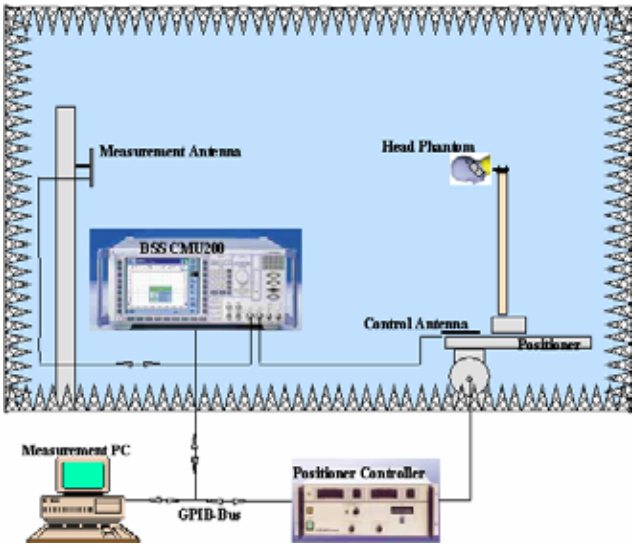

Figure 2. Measurement setup for active mobile phone measurements

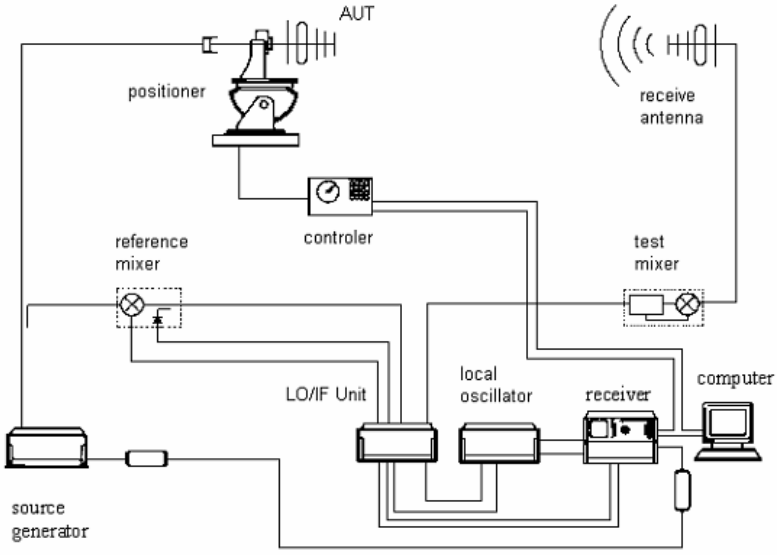

Figure 3. Standard setup for passive antenna measurement

Evaluation

The evaluation can provide the following items:

- An intensity diagram
- Three polar diagrams, which show the radiation characteristics in the main planes (XY-, XZ- and YZ-planes)
- The values of TRP, EIRP or TIS and EIS.

Figure 4 shows the coordinate systems used for the evaluation, for different measurement cases.

The information contained in this document should be used only for the scope of the contract for which this document is prepared.

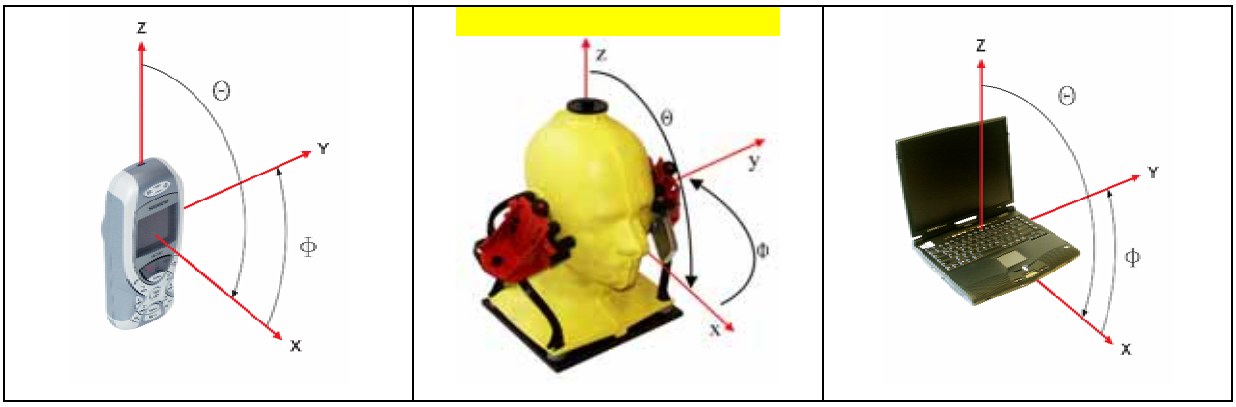

Figure 4. Coordinate system for different measurement cases: mobile phone (left), mobile phone with user's head (centre) and laptop (right)

Intensity Diagram

The intensity diagram shows the measured values in a Cartesian coordinate system. The axes correspond to the ϕ and θ coordinates, the measured intensity is represented by the colours. Figure 5 shows as an example of the intensity diagram for a mobile phone in the GSM 900 band.

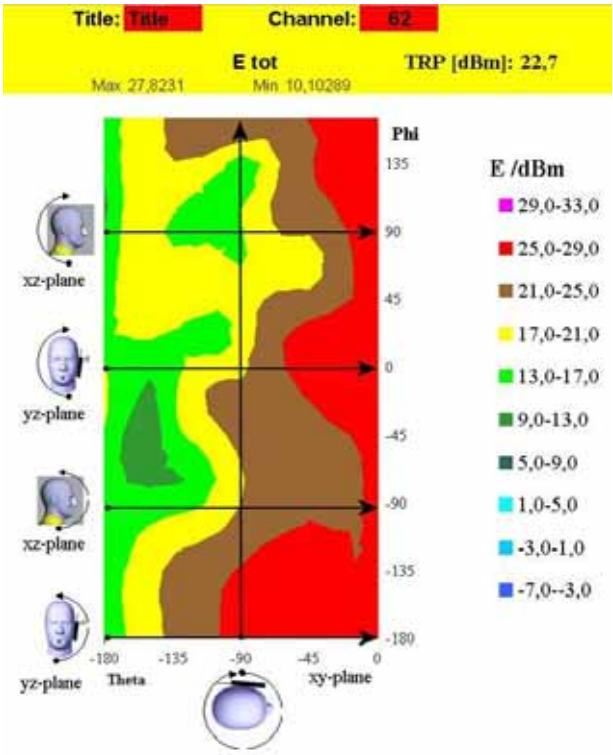

Figure 5. θ-ϕ intensity diagram with head phantom in the GSM 900 mode.

Polar diagram

The polar diagrams represent three differect cuts of the radiation pattern, corresponding to the three main planes: the horizontal xy-plane (θ = 90°), the vertical xz-plane (ϕ = 0°) and the second vertical plane, yz-plane (ϕ = 90°).

The information contained in this document should be used only for the scope of the contract for which this document is prepared.

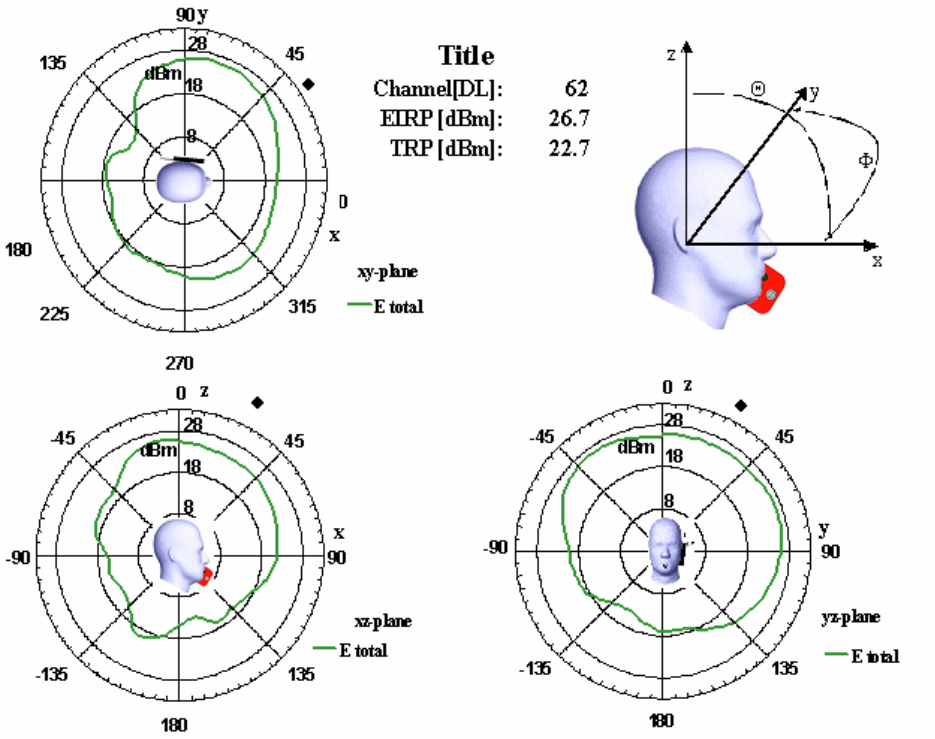

Figure 6. Polar diagrams: upper left xy-plane, lower left xz-plane, lower right yz-plan

5.1.2 Spherical Near Field Antenna Measurements

Antennas are generally operating under conditions which put the receiving and transmitting antennas at large distances from each other. At long distances, the angular variation of the electromagnetic radiation is not a function of the distance and we name this the far-field of the antenna. Antennas are generally characterized by this far-field radiation pattern. The commonly used criterion to determine the distance before the far-field radiation pattern is obtained corresponds to $2D^2/\lambda$. For bigger antennas, this far-field distance can be so large that indoor facilities become impractical and unaffordable. For such reasons the space and military industries pushed for the development of compact indoor antenna test ranges. Two main configurations have become common, the near-field measurement systems, and the Compact Antenna Test Ranges. The near-field measurement systems involve the sampling of the field surrounding an antenna and using an exact numerical algorithm to transform this measured near-field into far-field radiation pattern. The Compact ranges on the other hand use large reflectors that convert the spherical phase front of a probe antenna to a pseudo plane wave which is incident on the antenna under test.

Near-field measurement techniques are a practical application of the Huygens's principle. This fundamental law of electromagnetics states that given only the electromagnetic fields due to one or more sources over a surface enclosing these sources, the field can be determined exactly everywhere outside this surface.

Since the middle of the 1970's when efficient electromagnetic algorithms where developed, Spherical Near-Field measurements have been recognized as a very accurate approach for the measurement of antenna radiation characteristics.

The information contained in this document should be used only for the scope of the contract for which this document is prepared.

For the spherical near-field case, the field radiated by an antenna is sampled over a spherical surface surrounding the AUT. The near-field to far-field transformation is performed by expressing the measured field in terms of spherical wave functions. Spherical wave functions are the natural solutions to Maxwell's equations expressed in spherical coordinates. The angular and radial variation of these functions are described by Legendre Polynomials and Spherical Hankel functions (or Bessel Functions), respectively. By finding the best set of coefficients for the series of spherical wave functions which match the measured field, we can efficiently evaluate the radiated field everywhere outside (and to some extent also inside) the measurement sphere [7].

5.1.3 STARGATE and STARLAB spherical near field measurement systems

The standard STARGATE system is a spherical near field test range imagined, developed and produced by SATIMO which uses a circular probe array to allow for real time full elevation cuts and volumetric 3D radiation pattern measurements within a few minutes (see *Figure 7*).

Figure 7. Spherical near field antenna test range with circular probe array (left) Instrumentation rack including synthesizers, receiver, probe array controller (right)

This measurement system is operating between 400 MHz and 6 GHz and can be configured for passive measurements and also cable-less active measurements.This system addresses the following issues usually complicating conventional measurement of small personal communication terminals [8]:

1. Omni-directional but complex beam shape antennas need characterisation over a full sphere. It has been common to only characterise the telephone radiation patterns for a few radiation pattern. But obviously, holes in the radiation pattern can occur outside one of these discrete cuts and a full 3-D pattern is required to fully characterise the telephone performances.

2. To avoid interactions with a positioner, all materials surrounding the phone are generally made out of a low dielectric constant material such as polystyrene. Even small wooden interface plates have been known to disturb the measurements

The information contained in this document should be used only for the scope of the contract for which this document is prepared.

significantly. A two-axes positioner with a low level of interaction is difficult to implement.

3. As the AUT is nearly omni-directional, it "sees" all the walls of the anechoic chamber. Thus, the design of the anechoic chamber has to rely on good absorbing materials down to 800GHz on all the surrounding walls. Especially the wall behind the AUT is a big contributor to measurement uncertainty.

4. One of the big error contributors to the radiation pattern measurements is the presence of the RF feed cable. Several solutions are used in industry to overcome this problem. One solution for passive measurements is a coaxial line loaded with ferrite in order to suppress the induced currents on the cable. Some experiments have also been performed using small CW sources integrated in the phone and using an auxiliary antenna at the base of the positioner to collect the reference signal. Finally, there is a great interest to perform cable-less active measurements using a standard phone as the source and a base station simulator to collect the signal.

5. Operators have different characteristics (glasses, helmets, exact positioning of the phone, etc.). The phones can to some extent be designed to reduce the detrimental effect of the presence of an operator. The standard procedure is to use a human model made in a plastic material and filled with a liquid simulating the dielectric constant of the operator. These models also called phantoms are never perfect replicas of a human operator and there is an interest in testing the telephone also using a real person. Measurements using a person are difficult on a two axes positioner. With a standard antenna measurement system the operator would have to be rotated in all directions, including upside down.

Another example is the STARLAB system [9] that probes the fields at 15 elevations simultaneously (see *Figure 8*). The AUT needs to be rotated only around the vertical axis. A full 3-D radiation pattern can be measured from 800 MHz to 6 GHz within a few minutes. The measurement radius of 45 cm is sufficient for measurements up to the PCS band, also in the presence of a phantom head.

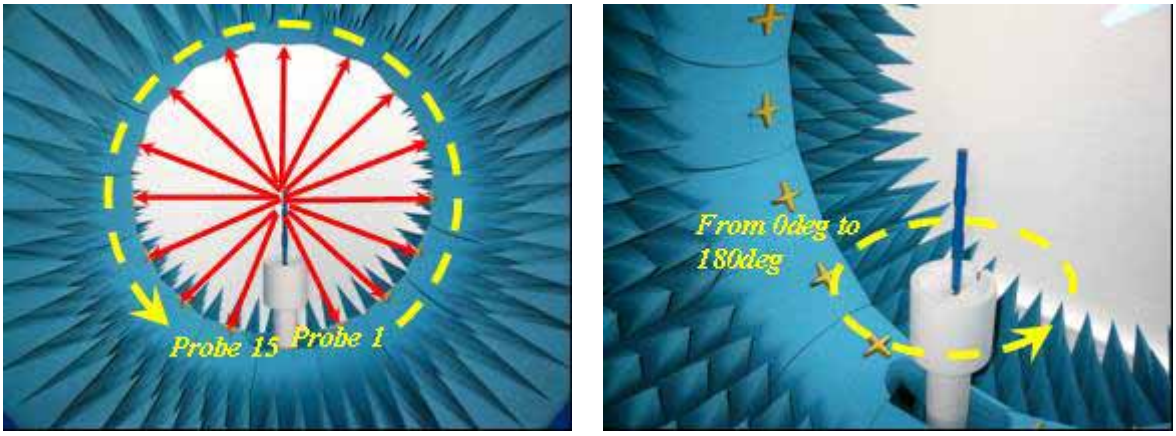

Figure 8. STARLAB multi-probe system(left: electronically scanned elevation; right: mechanically scanned azimuth)

The information contained in this document should be used only for the scope of the contract for which this document is prepared.

5.1.4 Spherical Angular Sampling Criteria

The Near-Field acquisition and Far-Field representation are made over a spherical surface roughly centered on the AUT. The used spherical angular samplings both in θ and ϕ are presented on Figure 9:

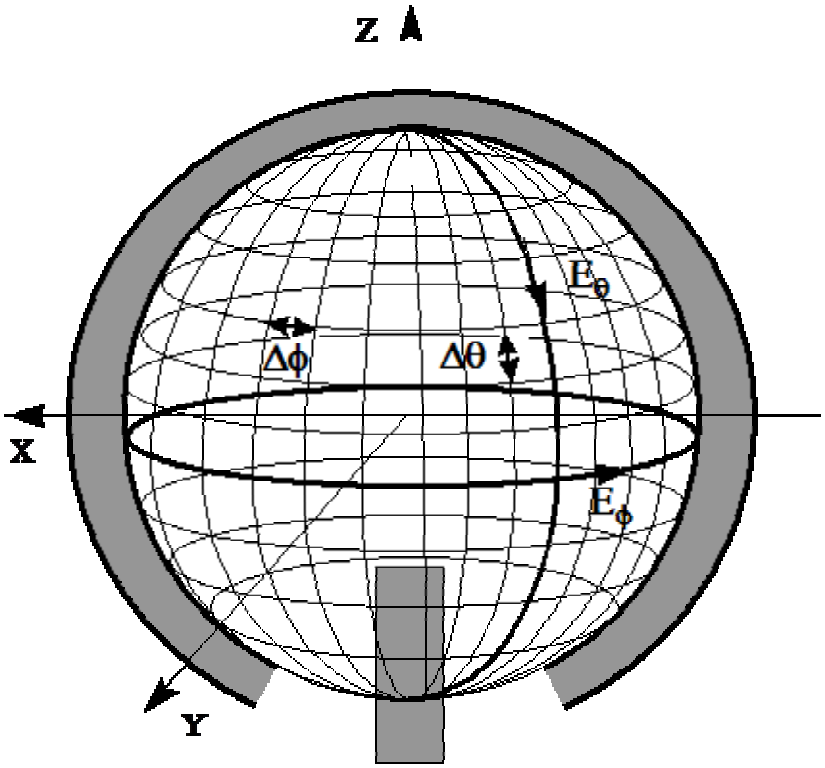

Figure 9. Spherical angular sampling in Spherical Near-Field Facility

During the acquisition of Spherical Near-Field data, three different sampling criteria can be used in regards with the theory of spherical mode expansion. The number of acquisition points in elevation is given for π radians. The sampling criteria are summarized in Table 1 below:

Sampling Criteria	Max Sample Spacing on Min. Sphere	Minimum Number of Samples (over π radians)	Maximum AUT Radius
Criterion A)	$(\frac{\lambda}{2})$	$N_\theta = \text{int}(kr_{min})$	$r_{crit} = \frac{N_\theta}{k}$
Criterion B)	$(\frac{\lambda}{e})$	$N_\theta = \text{int}((\frac{ek}{2})r_{min})$	$r_{crit} = \frac{2N_\theta}{ek}$
Criterion C)	$(\frac{\lambda}{2})$ – margin	$N_\theta = \text{int}(kr_{min}) + 10$	$r_{crit} = \frac{(N_\theta - 10)}{k}$

Table 1. Three different sampling criteria w.r.t. the spherical expansion theory

The information contained in this document should be used only for the scope of the contract for which this document is prepared.

Criterion A corresponds to a distance exactly equal to half a wavelength between sampling data if these are projected on the minimum sphere surrounding the object under test.

Criterion B corresponds to a distance equal to (λ/e) between sampling data if these are projected on the minimum sphere surrounding the object under test. The value of *e* is equal to 2.718281828

Criterion C corresponds to a distance lower than half wavelength between sampling data if these are projected on the measurement sphere, but a margin is taken to avoid very small number of modes for small antennas and/or low frequencies.

The angular increments in θ and ϕ can be deduced from the following formula :

$$\Delta_\theta = \Delta_\phi = \frac{\pi}{(N_\theta - 1)}$$

where $\Delta\theta$ is the increment in elevation and $\Delta\phi$ is the increment in azimuth.

The total number of acquisition points over an elevation range of π and an azimuth range of 2π is then given by :

$$N = N_\theta N_\phi = 2N_\theta (N_\theta - 1)$$

In the sampling data criteria, r_{min} denotes the radius of the smallest possible spherical surface (named minimum sphere) circumscribing the AUT.

As illustrated in Figure 10, it is important that the AUT is mounted so that the radius of the minimum sphere is as small as possible. This is obtained when the center of the minimum sphere coincides with the center of the *Spherical Near-Field Facility*, that is to say when the center of symmetry of the AUT coincides with the center of the *Spherical Near-Field Facility*.

The information contained in this document should be used only for the scope of the contract for which this document is prepared.

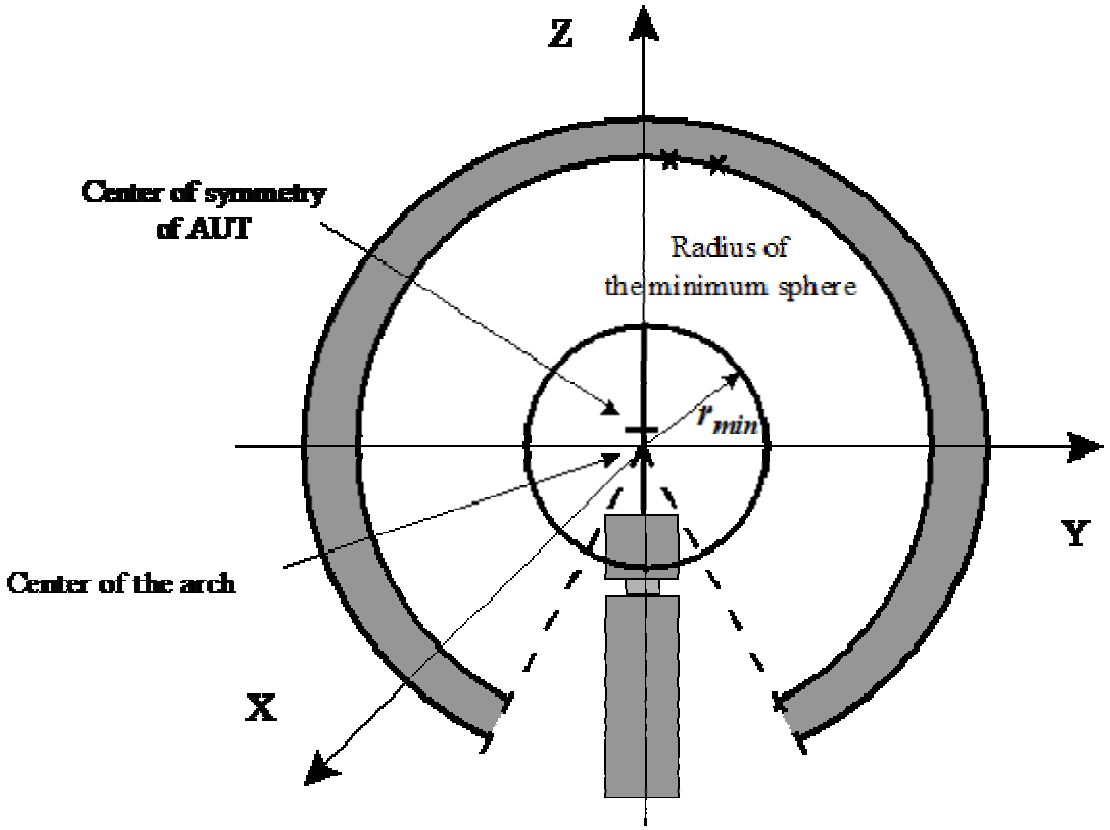

Figure 10. Definition of the radius of the minimum sphere.

The radius of the minimum sphere r_{min} must take into account the offset between the center of symmetry of the AUT and the center of the *Spherical Near-Field Facility*.

5.1.5 Definition of the maximum radius for the AUT

Since in the *Near-Field Facility*, the number of acquisition points in elevation N_θ and the increment in elevation $\Delta\theta$ are maintained constants, the maximum radius of the AUT depends on the frequency and the sampling criterion used. A second criterion that limits the maximum size of the AUT is the physical distance between the AUT and the test probes. To avoid the reactive field region and to reduce the interactions between the probes and the AUT it is advantageous to keep at least two wavelengths between the AUT and the probe. This criterion is thus written:

$$r_{meas} = r_{arche} - 2\lambda$$

From *Table 1* it is obvious that the criterion radius r_{crit} increases when the frequency decreases. On the contrary, r_{meas} decreases when the frequency decreases. At low frequency, the criterion radius r_{crit} can be greater than the physical radius r_{meas}. Then, the lower values between both criterion radius constitute the maximum authorized radii which are given in Table 2 below.

The information contained in this document should be used only for the scope of the contract for which this document is prepared.

frequency	0.8 GHz	1.0 GHz	1.5 GHz	2.0 GHz	2.5 GHz	3.0 GHz	3.2 GHz
Criterion A							
r_{max}	0.85 m	1.00 m	1.18 m	0.88 m	0.71 m	0.59 m	0.55 m
Criterion B							
r_{max}	0.85 m	1.00 m	0.87 m	0.65 m	0.52 m	0.43 m	0.41 m
Criterion C							
r_{max}	0.85 m	1.00 m	0.86 m	0.64 m	0.52 m	0.43 m	0.40 m

Table 2. Maximum authorized radii for the AUT depending on the criterion A, B or C and on the frequency in the case of a STARGATE64 measurement system (no elevation over-sampling used).

To be in accordance with criteria A, B or C, the *Spherical Near-Field Facility* User must respect the calculated maximum authorized radii for the AUT. The maximum authorized radius values guarantee that the acquisition of the Spherical Near-Field data will be sufficiently sampled in order to provide accurate Far-Field Test Parameters of the AUT.

5.1.6 Example of passive measurements of omni-directionnal antennas

In order to assess the accuracy on the measured radiated power of isotropic-like antennas, a reference dipole placed in the center of the arch has been measured for different loss-less configurations (dipole straight or tilted, dipole with a plate straight or tilted, etc.). The measurements have been performed at 900 MHz and 1800 MHz which are representative frequencies for future measurements of mobile phones. The measurement set-up and some examples of measured 3D radiation pattern at 1800 MHz are shown in Figure 11. The measured efficiency for the different configurations dipole / plate are summarized in Table 3 after correction of the return loss variation. The results obtained (statistical one sigma efficiency of 1.17% at 900 MHz and 0.69% at 1800 MHz) are demonstrating the well suitability of the system at measuring isotropic-like and mobile phone antennas.

The information contained in this document should be used only for the scope of the contract for which this document is prepared.

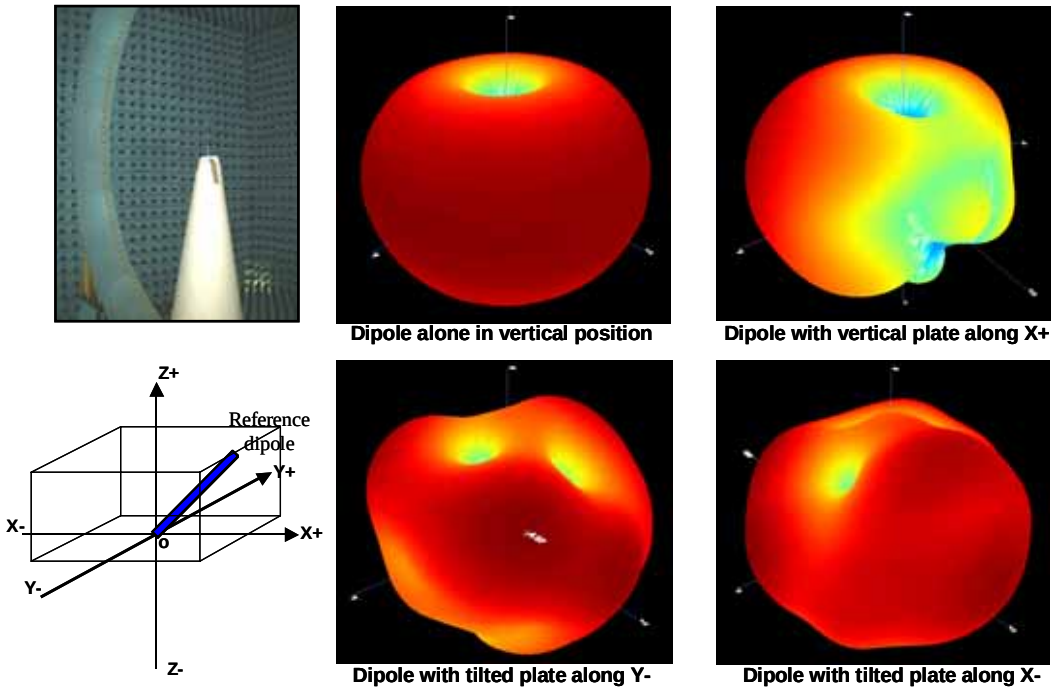

Figure 11. Measured radiation pattern of dipole at 1800 MHz for different configurations dipole / plate.

Configuration	corrected η
Dipole alone	97.20 %
Dipole at 45° along Y-	99.00 %
Dipole at 45° along X-	98.60 %
Dipole at 45° along Y+	98.50 %
Dipole at 45° along X+	98.30 %
Dipole + vertical plate Y-	96.55 %
Dipole + vertical plate X-	96.55 %
Dipole + 45° tilted plate Y+	96.58 %
Dipole + 45° tilted plate X+	95.88 %

Configuration	corrected η
Dipole alone	96.92 %
Dipole at 45° along Y-	97.72 %
Dipole at 45° along X-	97.32 %
Dipole at 45° along Y+	97.22 %
Dipole at 45° along X+	97.02 %
Dipole + vertical plate Y+	97.90 %
Dipole + vertical plate X+	98.00 %
Dipole + 45° tilted plate Y-	98.78 %
Dipole + 45° tilted plate X-	98.68 %

Table 3. Measured efficiencies at 1800 MHz (left) and 1800 MHz (right) for different configurations.

5.1.7 Configuration of active measurements

The STARGATE system can measure mobile phones in active mode thanks to optional hardware and software [10]. Such measurements are achieved via a radiocommunication tester (base station simulator). This device is capable of initiating a call to a mobile under test and measuring the two-way communication link for different communications standards and frequencies. To interface this test equipment to the STARGATE system, an Active Measurement Test Unit (AMTU) is also required. This piece of hardware contains a series of switched amplifiers and filters that will compensate for the additional free-space losses and probe array losses that are present in a typical STARGATE measurement configuration.

The information contained in this document should be used only for the scope of the contract for which this document is prepared.

During this test mode, two-way communications is established through the probe array and both Transmit and Receive channel parameters are obtained. A block diagram of the system is shown in *Figure 12* and *Figure 13* for TRP and TIS measurement configurations, respectively. The Probe Array Controller is used to control the probe array and to sequentially select the probe and polarization to be measured. The radiocommunication tester establishes a two-way link to the mobile phone through the AMTU and Probe Array. It is then possible to record the link parameters as reported by the tester for each probe and polarization angle.

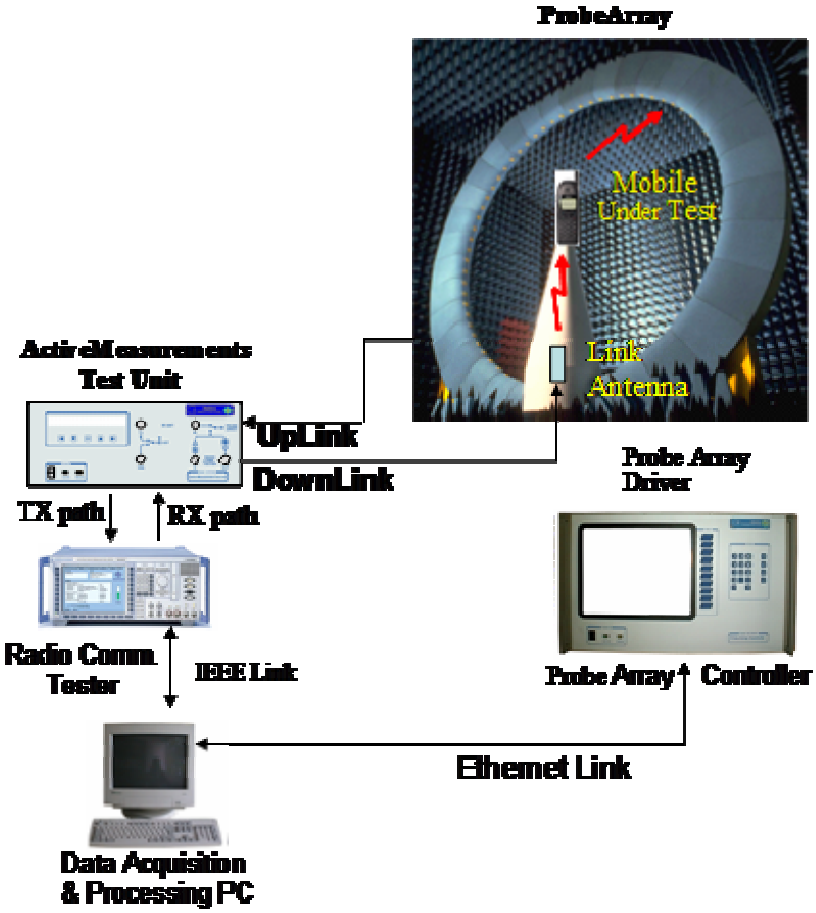

Figure 12. Functional Block Diagram showing the STARGATE configured for TRP measurements.

The information contained in this document should be used only for the scope of the contract for which this document is prepared.

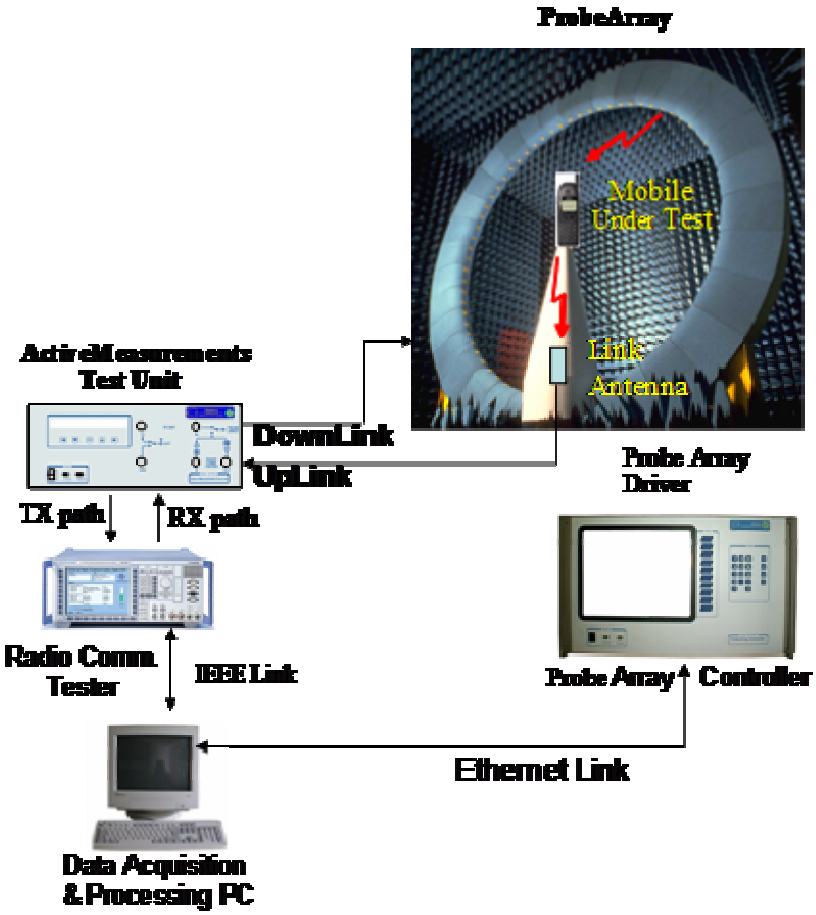

Figure 13. Functional Block Diagram showing the STARGATE configured for TIS measurements.

5.1.8 Example of active measurement results

The active measurements of mobile phones in a STARGATE system allow the user to characterize the radiation pattern of the mobile under test over a full sphere. The user is able to visualize the 3D pattern or the 1D views for the main E-plane and H-plane cuts (see typical measurement results in *Figure 14*). The power transmitted by the phone as well as the power received by the phone can be measured.

Typically the power transmitted by the phone (Tx power) will be measured for different channels (i.e. different frequencies). From the measured EIRP data (Effective Isotropic Radiated Power), the TRP (Total Radiated Power) and the efficiency are determined. In terms of power received by the phone (Rx power), the system can measure the sensitivity of the phone. In this case, the system will decrease the level incoming from the base station simulator until reaching a certain level of the Bit Error Rate corresponding to the sensitivity level. From the measeared EIS (Effective Isotropic Sensitivity), the TIS (Total Isotropic Sensitivity) is determined.

The information contained in this document should be used only for the scope of the contract for which this document is prepared.

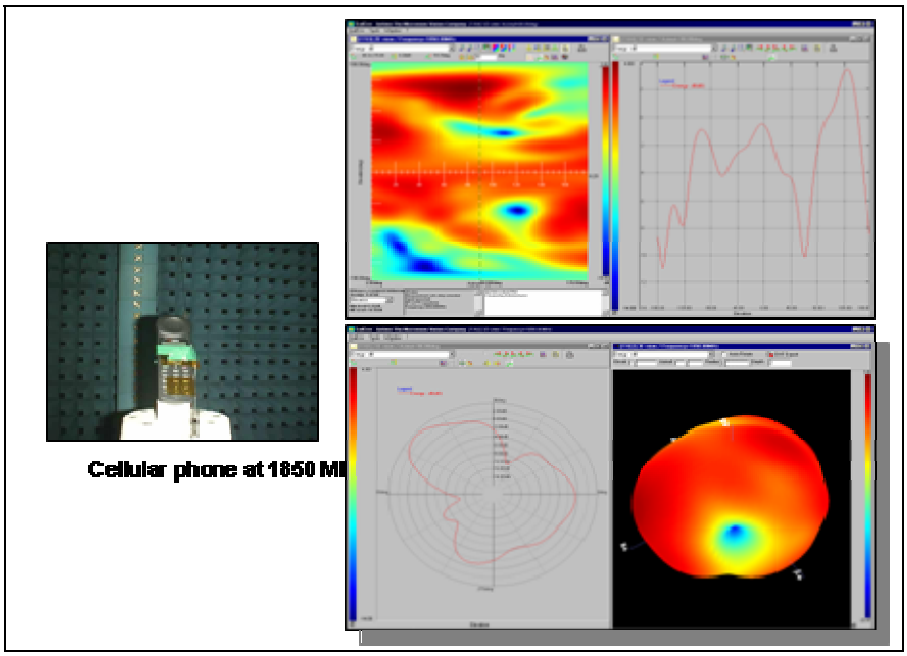

Figure 14. Active measurement results of mobile phone in DCS frequency band (2D-plot, 1D-cut and 3D-view).

5.1.9 Human body interaction

Due to the rapidity of the measurements in the STARGATE system, it is possible to characterize a real person in communication and not only a phone mounted on a phantom. SATIMO has developed a special seat with armrest dedicated to this kind of measurements, thus allowing a good repeatability of the measurements. The *Figure 15* shows a configuration of an active measurement performed in free space with a human operator. The radiation pattern containing the effects of the human body interactions with the phone is displayed in *Figure 16*. In the same Figure, this radiation pattern is compared to the radiation pattern of the single phone measured separately.

Figure 15. Active measurement results of a GSM mobile phone measured in free space and with user.

The information contained in this document should be used only for the scope of the contract for which this document is prepared.

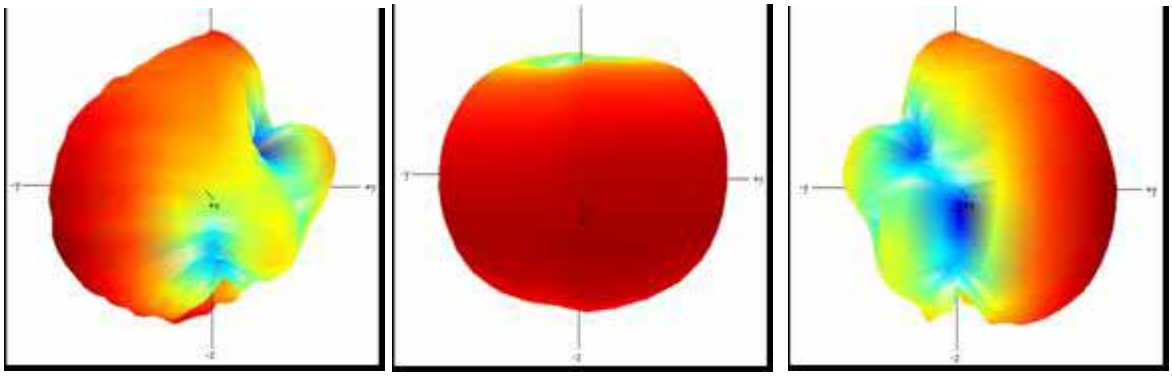

Figure 16. Measured active radiation pattern without (middle) and with the presence of a human operator (right: Head right ear; left: Head left ear).

5.1.10 Alternative 3-D field measurement system

An alternative 3-D field measurement system is capable of measuring the radiation pattern of a mobile-terminal antenna without rotating the terminal at all [9]. The system operates 800 MHz to 3 GHz, and simultaneously measures both polarizations of the radiated fields at 32 locations on a spherical surface with 1m radius (Figure 17), allowing for a head model or a real user to be included. The measurement time for a complex 3-D pattern at one frequency is 4 s. The spherical wave expansion technique is used to determine the complex far field based on these 64 field samples (measurement channels). The phase of the radiated fields is determined by a phase-retrieval network that uses one particular measurement channel as a phase reference to determine the relative phase of all other 63 measurement channels. This facilitates measurements of the complex radiation properties of active mobile terminals without the need to attach an RF cable to the mobile terminal.

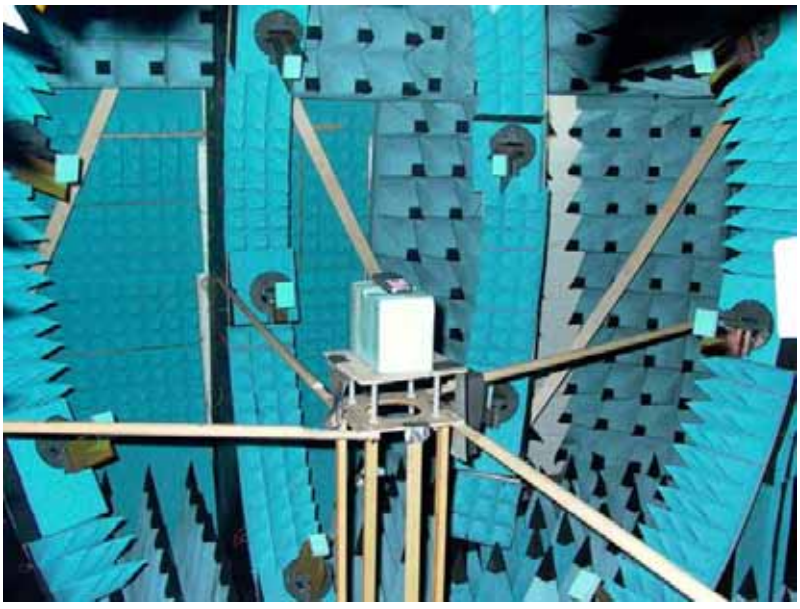

Figure 17. A spherical multi-probe system.

The information contained in this document should be used only for the scope of the contract for which this document is prepared.

In several measurements with small antennas the size of typical mobile terminals, in the frequency range of 900 MHz to 2.5 GHz, it was found that the retrieved phase patterns agree very well with the directly measured phase pattern (in an anechoic chamber) up to 2 GHz, and acceptably above 2 GHz. Also the amplitude patterns agree very well below 2 GHz and relatively well above 2 GHz. The repeatability of the measurements was around +/- 0.1 dB for 900 MHz and gradually increased to about +/- 1 dB at 2.5 GHz. It was expected that the uncertainty increases with frequency, since due to the relatively small number of measurement locations (32), the measurement accuracy of RAMS is dependent on the size of the AUT in wavelengths.

5.1.11 Radio-Channel sounder measurements

Especially for multi-element antennas as used in MIMO systems, it is important to obtain realistic performance data in their real usage environment. A channel sounder with multiple transmitter and receiver channels can give a good figure of merit for the statistical characteristics of a multi-element antenna [11], especially the Mean Effective Gain [12] and the Channel Capacity (see Ch. 4.7).

However, when comparing different antenna configurations, several hundred meters of measurement routes in the several types of propagation environments would needed for each prototype antenna to obtain statistically significant results. This is difficult due to the large amount of measurements needed. It would be useful to test the performance of new multi-antenna mobile terminals in real signal propagation environments already during the early simulation phase of the design process. A new plane-wave based method for multi-antenna performance evaluation fulfills exactly this requirement [13].

The plane-wave based method is based on the joint contribution of a) the estimate of the distribution of incoming signals (complex envelope, direction of arrival, delay) in the propagation environment, and b) the complex 3-D radiation patterns of terminal antenna. The complex 3-D radiation pattern of the antenna under test can be simulated by using software or measured in an anechoic chamber (see Ch. 5.1). Component-wise multiplication and summing up of the two contributions gives the total received signal. The importance of this method comes from the fact that with a large database of measured radio channels it is possible to predict the diversity or MIMO performance of new multi-antenna designs even before a prototype is available, since the simulated radiation patterns can be used, i.e. no measurements are necessary. The required channel databases are already available at several research institutes and companies.

The information contained in this document should be used only for the scope of the contract for which this document is prepared.

5.2 Reverberation chamber

The reverberation chamber has been used for EMC testing for a couple of decades. The last four years its capabilities have been extended to accurate measurements of small antennas and active terminals that are designed for use in Rayleigh fading environment.

The reverberation chamber is a metal cavity which is large enough to support several cavity modes at the frequency of operation. The modes can be stirred to create a Rayleigh distributed transfer function between two antennas inside the chamber [14]. The Q of the chamber is affected by wall losses, leakage, lossy objects as well as the antennas, and can be used to control the average power level of the transfer function [15]. This average level is produced by measuring the transfer function for several stirrer positions and averaging these levels. Reverberation chambers with high Q have for a couple of decades been used for EMC measurements [16]. The Rayleigh statistics is also present in chambers with low Q (down to 100). This makes them possible to use for testing of mobile terminals designed for use in fading environments.

Measurements in a reverberation chamber are performed by measuring the transfer function between an antenna or terminal under test and some fixed wall antennas. When the power of this transfer function is averaged over the stirrer positions, the averaged level is proportional to the radiated power of the terminal under test or the radiation efficiency of the antenna under test [15]. The work to make the reverberation chamber a practical measurement instrument for mobile terminals started by developing a small chamber which could be used with reasonable measurement accuracy (0.5 dB standard deviation of average levels of transfer function) down to 900 MHz (Figure 18). This was enabled by more field stirring methods than those used before, which were limited to mechanical stirring and frequency stirring [16], the new methods being referred to as platform stirring [17] and polarization stirring [18]. The standard size chamber shown in the figure is moveable on wheels (when lifted down from its support frame), and it can pass through a door of 80 cm width. The chamber can also be extended to larger widths and heights. The chamber comes today with control software for the different types of measurements described below.

The information contained in this document should be used only for the scope of the contract for which this document is prepared.

-

Figure 18. The Bluetest reverberation chamber shown with open door with a setup for measuring radiated power of mobile phone close to head phantom. The chamber size shown can be used for measurements down to 850 MHz.

Radiation efficiency measurements
The average transfer function of the chamber is proportional to the radiation efficiency of the antennas [15]. Therefore, the chamber can be used to measure radiation efficiency by comparison with a calibration antenna with known radiation efficiency. The radiation efficiency includes contributions due to input port reflections [19].

Total radiated power of mobile terminal
The measurements of total radiated power of mobile phones in "free space" position as well as different talk positions close to a human head is described in [20], [21]. This way of measuring total radiated power is included in the TCO'01 Mobile Phones quality labeling [22]. The procedures have been extended to mobile systems of different standards, also Bluetooth [23].

Apparent, effective and actual diversity gain
Antenna diversity is allowed in UMTS, CDMA2000 and some Japanese and Korean systems. This requires special measurements to be able to quantify and optimize the antenna performance. The reverberation chamber is well suited for this as its environment has a similar Rayleigh distribution as actual urban and indoor environments for mobile communication. The measurement procedures as well as theories for antenna diversity have been developed [24], [25], [26], [27].

Diversity gain of active terminals
The reverberation chamber is in particular attractive for measuring implemented diversity gain in active terminals, such as in the measured DECT phones described in [28]. The measured results from the latter are shown in Figure 19. We see that the implemented diversity in the phone gives a diversity gain of 5 dB at 1% cumulative level, compared to the level when the strongest antenna (diversity branch) is used. The maximum available diversity gain from the two implemented antennas in the phone when selection combining is used is seen to be 2 dB larger.

The information contained in this document should be used only for the scope of the contract for which this document is prepared.

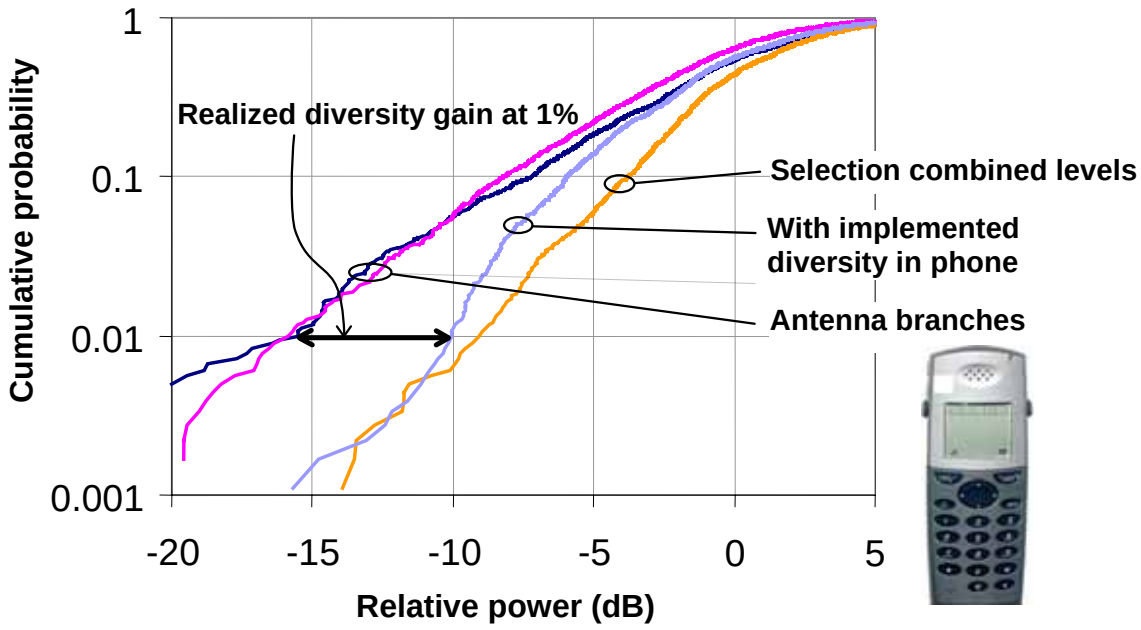

Figure 19. Cumulative distribution of signal amplitudes when an active DECT phone with implemented antenna diversity is used in reverberation chamber. The inserted "↔ line" shows the implemented diversity gain, which is about 2 dB lower than the theoretical maximum by selection combining.

Receiver sensitivity of active terminals

The quality of a received signal in a mobile terminal is characterized by the bit error rate (BER), or by the corresponding frame error rate (FER) in CDMA systems. The sensitivity is normally quantified in terms of the input signal level at a certain BER or FER level, for FER often chosen to be 0.5%. This sensitivity will depend on the level of the radiation pattern in the direction of the incoming wave. Therefore, it is common to specify a so-called total isotropic sensitivity (TIS) that is the averaged of this sensitivity over all directions of incidences of waves. This is equal to the sensitivity in dBm measured directly on the receiver input port, degraded by the radiation efficiency of the antenna. The TIS can be measured both in an anechoic chamber and in a reverberation chamber, but the procedure is laborious. The reverberation chamber offers in addition the possibility of a much faster measurement in an actual fading environment, with a continuously fading signal present at the terminal. This is a way of characterizing mobile terminals on reception which is very realistic compared to an actual operation of the terminal. However, this Average Fading Sensitivity (AFS) gives a larger dBm value than TIS (for the same BER or FER). The difference seems to be constant in dB, and we are working to theoretically evaluate this constant. At the moment it is sufficient to point out that the differences (in dBm) between the AFS of different phones seem to be the same as between the TIS of the same phones, see Figure 20. More results can be found in [2]. A mobile communication tester is needed for both TIS and AFS measurements.

The information contained in this document should be used only for the scope of the contract for which this document is prepared.

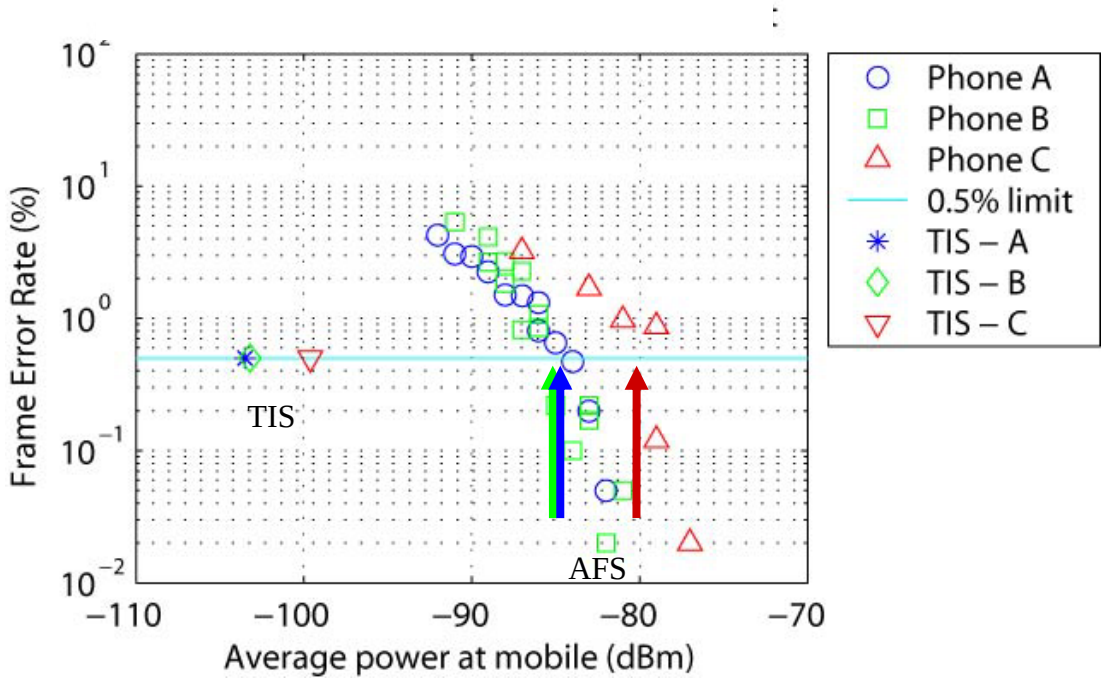

Figure 20. Frame Error Rates (FER) measured in reverberation chamber for three different CDMA2000 phones A, B and C, where phones A and B are the same model. The AFS levels of the three phones are marked with red arrows (where the three FER curves pass the 0.5% level). These are to be compared with the three marks to the left, corresponding to the TIS levels at 0.5% level. The difference between the TIS and AFS levels of the three phones are the same.

Terminals for future diversity and multiport MIMO systems

There is presently a lot of attention given to the research on future communication systems which continuously adapt to fading. A popular candidate for such is a so-called MIMO system (Multiple Input Multiple Output), where multiple ports on both the transmitting and receiving sides are used to generate several communication channels between which the signals are distributed in an optimum manner. MIMO antennas and terminals require special testing instrumentation. The quality of a MIMO system in a fading multipath environment is characterized by the maximum available capacity in bits/sec/Hz. Antennas for MIMO systems degrade the capacity due to both their radiation efficiency and correlation between received signals, of which the former is a dominating factor. The reverberation chamber offers a unique opportunity to experimentally characterize MIMO systems in a controllable fading environment. Results of such characterizations are already being published and compared with theoretical results [26], [27]. Some comparison between such measurements and numerical computations are shown in Figure 21.

The information contained in this document should be used only for the scope of the contract for which this document is prepared.

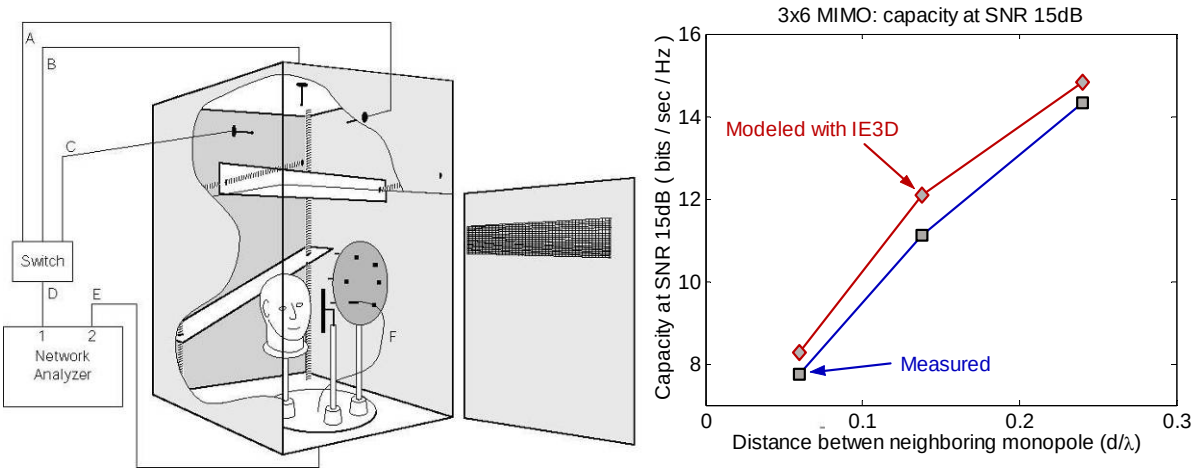

Figure 21. Experimental setup for measuring maximum capacity of a 3X6 MIMO system in a reverberation chamber. The antennas on one side are the three orthogonal wall antennas of the chamber, and on the other side 6 monopoles located along a ring on a circular ground plane. The measured capacity in the reverberation chamber are compared with theoretical values obtained by antenna simulations in a commercial code based on the embedded element patterns.

The information contained in this document should be used only for the scope of the contract for which this document is prepared.

5.3 Wheeler Cap Method

The Wheeler Cap method can only be used for electrically small antennas, since the antenna under test needs to fit inside the cavity.

Wheeler introduced a method for determining the radiation efficiency of antennas by performing two measurements, the first one in free space and the second one within a closed sphere [29] (Figure 22). He assumes, that the antenna at resonance frequency can be modelled as two series resistances; the radiation resistance R_{rad} and the loss resistance R_L. The first measurement delivers the sum of both contributions R_{free}, the second measurement delivers R_{cap}, which corresponds to R_L.

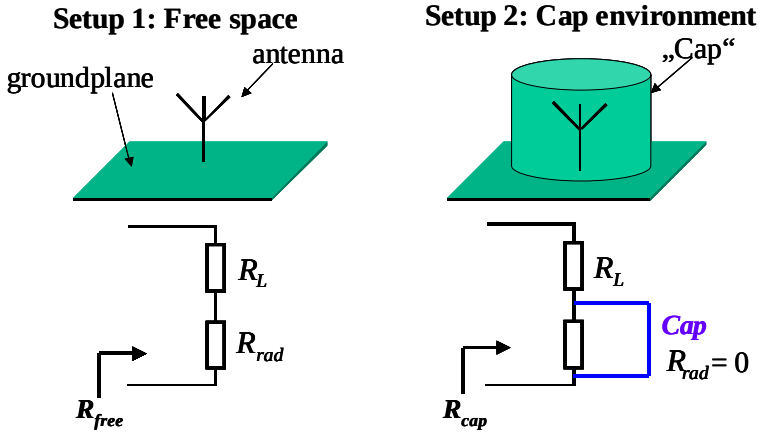

Figure 22 Wheeler-cap measurement procedure.

The method works under the assumption that the current distribution (and internal loss mechanism) of a small antenna will not be significantly disturbed when the antenna is placed inside a metal cap (i.e. with surface resistance R_s » 0). The cap then eliminates all radiation and thus also eliminates the radiation resistance R_{rad} . To obtain accurate results, cavity resonances must be avoided [30]. The loss resistance R_L is assumed to remain (practically) unchanged inside the cavity. In practice, the current distribution and thus also the resonant frequency of the antenna under test inside cap change slightly, typically leading to an uncertainty of several percents in the measured radiation efficiency. However, in practise the cap is not an ideal short circuit, but introduces new loses that can be taken into account using improved models [31]-[33].

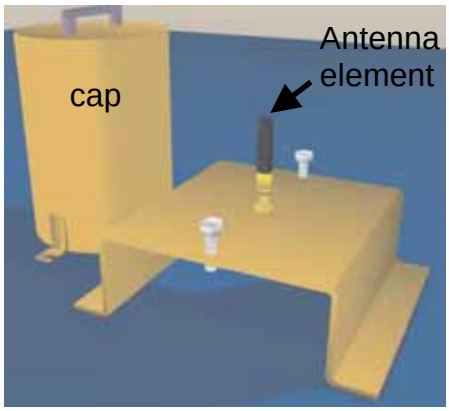

Figure 23. Wheeler cap measurement setup

The information contained in this document should be used only for the scope of the contract for which this document is prepared.

Under these conditions the radiation efficiency can be determined by performing two different measurements:

1. measuring the input resistance in free space ($R_{free} = R_{rad} + R_L$),
2. measuring the Antenna Under Test inside the cavity ($R_{cap} = R_L + R_s$)

To perform these measurements, a network analyser is used. The values of the input resistance with and without the cap can be obtained from the S-parameters of the antenna under test.

The **radiation efficiency** η_r can then be calculated as [34]:

$$\eta_r = \frac{R_{rad}}{R_L + R_{rad}} = \frac{R_{free} - R_{cap}}{R_{free}}$$

The total efficiency can be obtained by taking into account the input return loss at the feed point of the antenna:

$$\eta_{total} = \eta_r \left(1 - |S_{11}|^2\right)$$

Figure 24 shows some examples of the implementation of Wheeler-caps for the measurement of small terminals and small antennas.

Figure 24: Wheeler-cap measurement setups.

The information contained in this document should be used only for the scope of the contract for which this document is prepared.

5.4 Measurement of electrically very small antennas

The gain of electrically very small antennas is usually very low, and is governed by physical constraints [35]. Such antennas cannot be considered as purely symmetrical or purely antisymmetrical, due to the limited size ground plane and to the difficulty to properly realize baluns in a very small volume. The consequence is that classical antenna measurement techniques are no longer adequate, because of the current flow on the cable connecting the antenna to the measurement equipment [36]. In some cases, the gain might be overestimated by as much as 10 dB ! Furthermore, the radiation not only proceeds from the antenna, but also from the equipment casing on which the antenna is mounted. To complicate the problem, the polarization is seldom well defined.
In such conditions, the only way to obtain an accurate gain measurement is to test the antenna under operating conditions (mounted on the actual device case), and to insert a miniature battery-powered generator inside this (shielded) case. Of course, the generator (VCO) has to be tuned to the antenna resonant frequency, and its power level must be accurately known as a function of frequency. Furthermore, the battery capacity has to be sufficient to maintain a constant power level during the complete measurement period.
In most cases, one is looking for the maximum gain of the antenna under test. That means that the antenna has to be rotated in every possible angular position, with every possible polarization (as this parameter is usually not precisely known). With classical antenna positioners new problems are encountered: the positioner should provide at least a 3-axis rotation (azimuth, elevation and polarization), and should not cause any reflection in the vicinity of the small antenna, which has to be rotated in the whole space with every possible polarization. However, all commercial positioners are metallic and cannot be entirely covered with absorbing material. Moreover the antenna should be attached to the positioner, and this attachment point might perturb the antenna radiation, because small antennas radiate mostly omnidirectionnaly.

A solution to this difficult problem has been found. It consists of:

- Mounting the electrically small antenna under test in its definitive environment (on the shielded case which will later contain the electronic equipment used for the particular application).
- Feeding the antenna with a stable VCO of known (measured) output power, enclosed, together with batteries, in the shielded case. This forms the Device Under Test (DUT).
- Rotating (in an anechoic chamber) the DUT in all possible orientations and polarizations using a specially-designed "random" positioner, and capturing the maximum maximorum received level using the "peak hold" function of a spectrum analyzer.
- Replacing the DUT by a reference antenna having an accurately known gain and fed by a calibrated synthesizer at the same frequency as the DUT. The synthesizer power level is adjusted to obtain the same received level as the maximum produced by the DUT.
- The exact maximum gain of the small antenna under test can then be determined immediately by a simple calculation.

The information contained in this document should be used only for the scope of the contract for which this document is prepared.

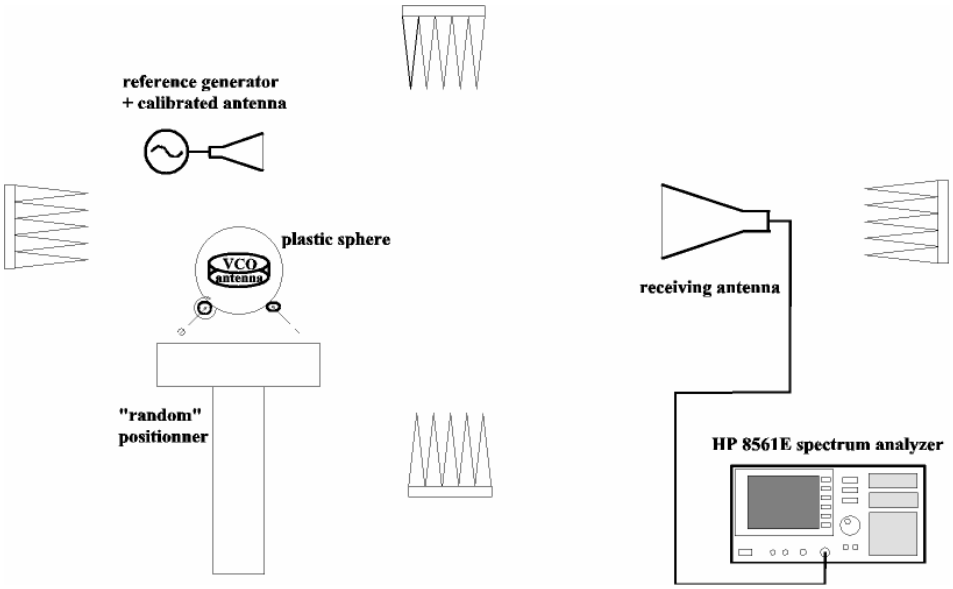

Figure 25. Principle of this measurement.

5.4.1 The “random” positioner

To position the DUT in every possible position and polarization, the idea is to enclose it within a dielectric sphere, which could be randomly rotated with a special device. As the DUT is small in our case, a 100 mm diameter Polypropylene sphere has been used. It has been modified so that it can easily be opened and closed to accommodate the DUT, which is centered within the sphere using low-density foam (see Figure 26).

Figure 26. DUT in sphere.

The goal in designing the special "random" positioner was to avoid any metallic part in the vicinity of the sphere. To do this, the sphere is placed on three 32 mm diameter wheels (Figure 27), each of them being powered by a compressed air "motor" (Figure 27). The

The information contained in this document should be used only for the scope of the contract for which this document is prepared.

orientation of each wheel is varied, at a different speed for each of them, using a fourth (electrical) motor enclosed within the positioner pedestal. The transmission of movement between this motor and the wheels is made with small driving belts, with a different speed for each of them (Figure 27). The speed of the three "motors" can be adjusted by varying the air pressure. The electrical motor velocity can also be easily varied.
The positioner is entirely made of plastic material (PVC, Polypropylene, Nylon), with the electrical motor as the single exception. But this motor is placed at the bottom of the system, about 50 cm away from the sphere containing the DUT.

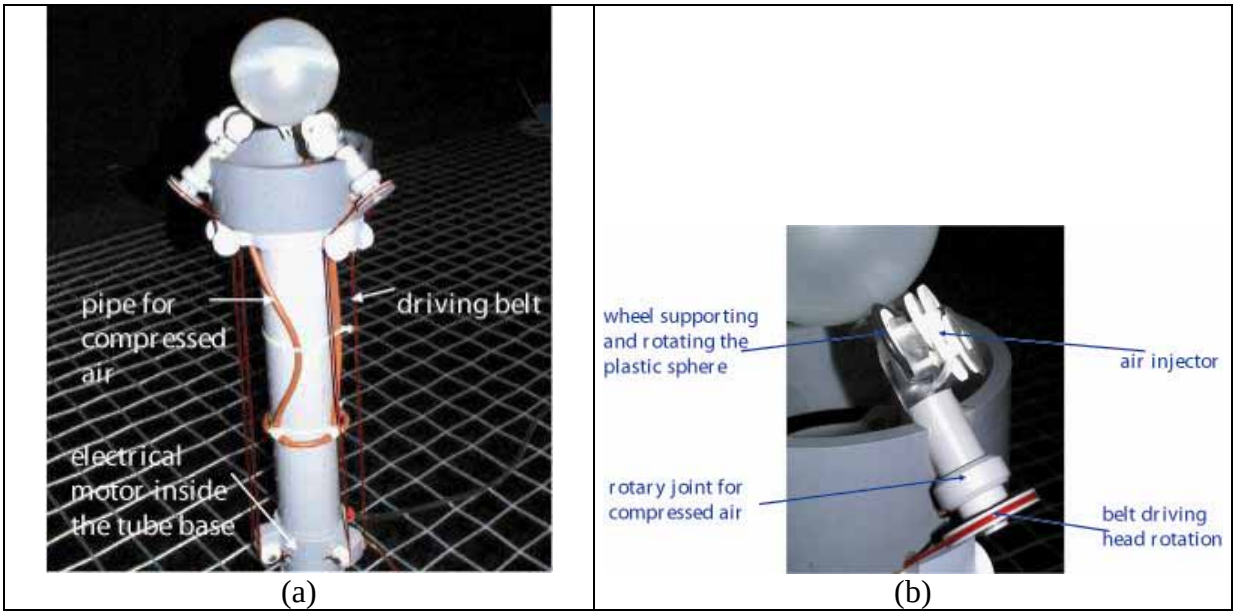

Figure 27. Positioner: General view (a) and detail (b).

With this approach, the movement of the sphere is completely random. It has been estimated from observations that a period of about 2 to 3 minutes is sufficient to scan the whole space.
Of course, the parameters of the spectrum analyzer used as a receiver have to be carefully adjusted (particularly the scan sweep) so that no peak in received power will be missed. With the slow movement of the sphere this is quite easy.

5.4.2 Example of measurement

A small antenna (35 mm total diameter, 10 mm thickness) designed for the 1.9 GHz band is measured with this system. The case enclosing the electronics is a 25 mm diameter brass case, completely shielded. The VCO output power is measured in the final configuration, without the antenna. The antenna is then mounted and connected. The entire system is shown in Figure 28, before the casing is closed

The information contained in this document should be used only for the scope of the contract for which this document is prepared.

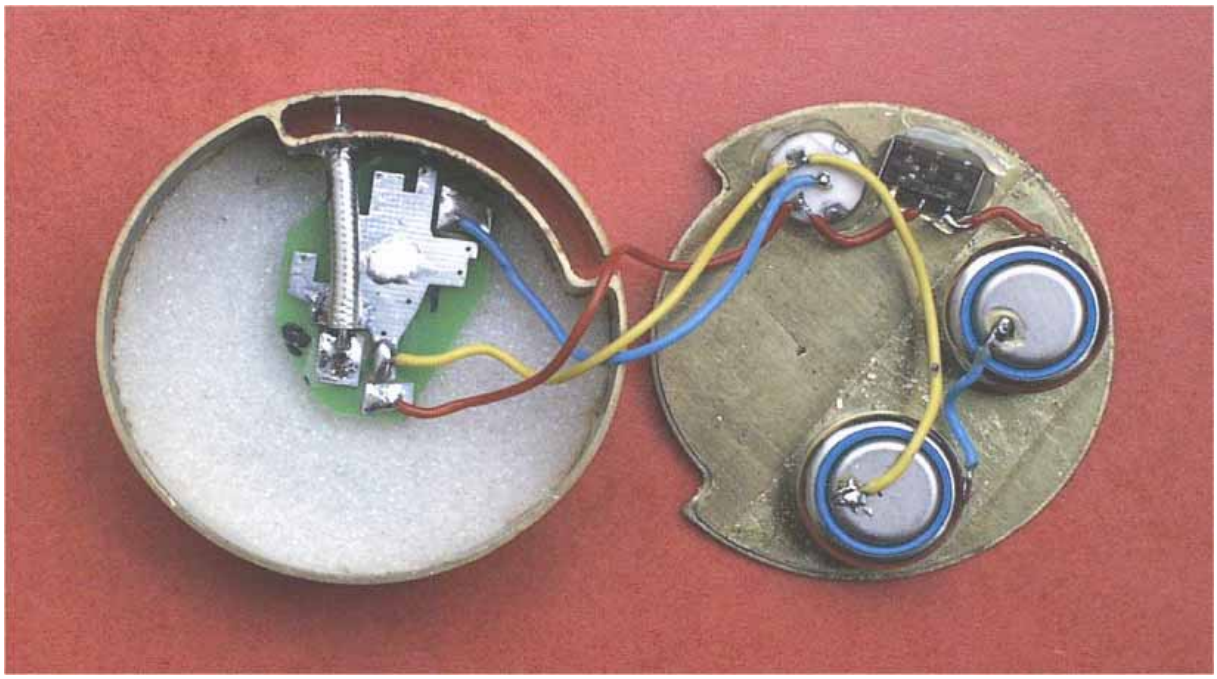

Figure 28. Integrated VCO and battery.

This complete DUT is then installed into the sphere. The sphere is put on the "random" positioner and the measurement can start : the spectrum analyzer is put in the "peak hold" mode, and one has to wait long enough so that the maximum doesn't increase any more. Usually, this takes about 2 to 3 minutes. The VCO is then switched off, and the sphere is replaced by the reference antenna (in our case a standard dipole mounted into an identical sphere, see Figure 29). With the spectrum analyzer in normal mode (peak hold OFF), the level of the calibrated synthesizer (tuned at the VCO frequency) is varied until the signal received on the spectrum analyzer is exactly the same level as previously. The gain of the unknown antenna can then be deduced immediately.

The information contained in this document should be used only for the scope of the contract for which this document is prepared.

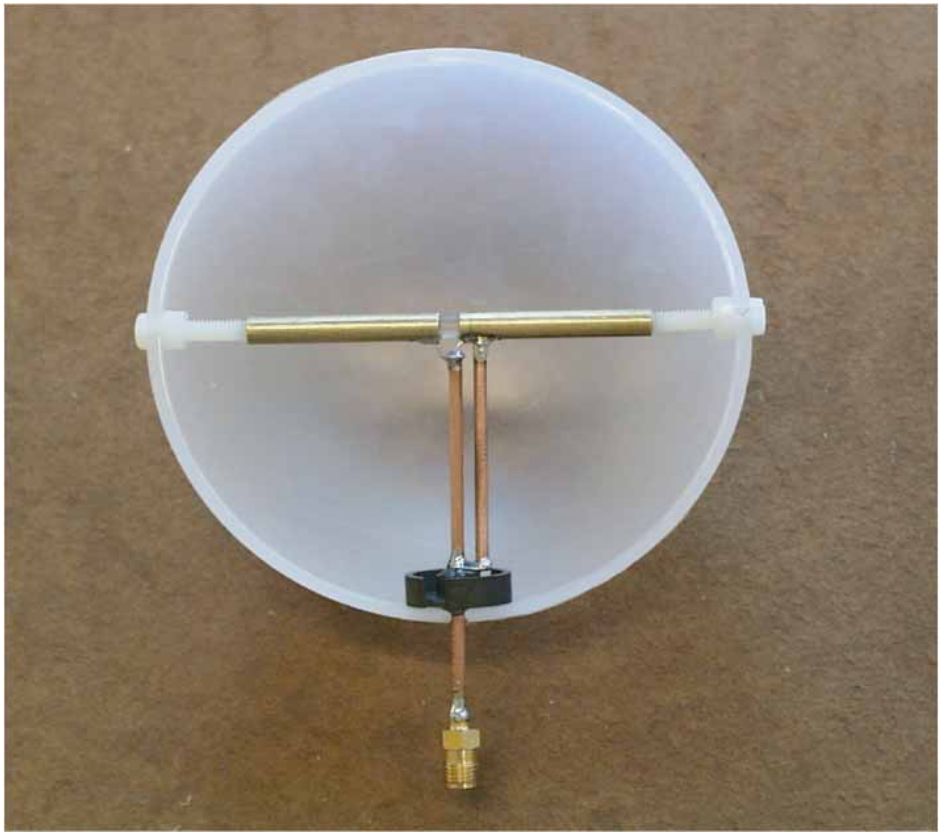

Figure 29. Example of reference antenna.

The information contained in this document should be used only for the scope of the contract for which this document is prepared.

6 References

[1] T. Taga, "Analysis for mean effective gain of mobile antennas in land mobile radio environments", *IEEE Transactions on Vehicular Technology*, 39(2): 117-131, May 1990.

[2] C. Orlenius, P.-S. Kildal, and G. Poilasne, "Measurements of total isotropic sensitivity and average fading sensitivity of CDMA phones in reverberation chamber", *IEEE AP-S Symposium, Washington DC*, July 2005 (Poilasne is with Kyocera).

[3] *"IEEE Standard Test Procedures for Antennas"*, ANSI/IEEE Std. 149-1979, IEEE Press, New York, NY, 1980, 143 pages.

[4] C. Icheln, J. Ollikainen, P. Vainikainen: 'The Effects of RF Absorbers on Measurements of Small Antennas in Small Anechoic Chambers', *IEEE Aerospace and Electronic Systems Magazine*, 11/01, pp. 17-20.

[5] http://www.ctia.org/

[6] *Test Plan for Mobile Station Over the Air Performance - Method of Measurement for Radiated RF Power and Receiver Performance*, Version 2.0, March 2003, CTIA Certification Department Program – www.ctia.org.

[7] Ph. Garreau, L. Duchesne, A. Gandois, J. Dréan, P.O. Iversen, "Antenna characterization solutions offered by using near field measurement techniques", 4th Mediterranean Microwave Symposium, Marseille 2004.

[8] P.O. Iversen, P. Garreau, K. Englund, E. Pasalic, O. Edvardsson, G. Engblom, "Real Time Spherical Near Field Antenna Test Range for Wireless Applications", Proceedings of AMTA 1999 – Antenna Measurement Techniques Association, pp. 363 – 368, October 4-8 1999, Monterey Bay, California.

[9] L. Duchesne, Ph. Garreau, N. Robic, A. Gandois, P.O. Iversen, G. Barone, "Compact multi-probe antenna test station for rapid testing of antennas and wireless terminals", 4th Mediterranean Microwave Symposium, Marseille 2004T. A. Laitinen, J. Toivanen, C. Icheln, P. Vainikainen: 'Spherical measurement system for determination of complex radiation patterns of mobile terminals', Electronics Letters, Vol. 40, No. 22, 10/04, pp. 1392-1394.

[10] A. Gandois, Ph. Garreau, G. Barone, "Active measurements of wireless devices in a spherical near-field test range", IEEE-AP, July 2001, Boston.

The information contained in this document should be used only for the scope of the contract for which this document is prepared.

[11] J. Kivinen, P. Suvikunnas, D. Perez, C. Herrero, K. Kalliola, P. Vainikainen, "Characterization system for MIMO channels," Proceedings of the 4th Int. Symposium on Wireless Personal Multimedia Communications, 2001, pp. 159-162.

[12] T. Taga, "Analysis for Mean Effective Gain of Mobile Antennas in Land Mobile Radio Environments," IEEE Trans. Veh. Technol., vol. 39, May 1990, pp. 117-131.

[13] P. Suvikunnas, K. Sulonen, J. Villanen, C. Icheln, P. Vainikainen, "Evaluation of performance of multi-antenna terminals using two approaches", Proceedings of the 21st IEEE Instrumentation and Measurement Technology Conference IMTC 2004, Como, Italy, May 2004, Vol.2, pp. 1091-1096.

[14] J. G. Kostas and B. Boverie, "Statistical model for a mode-stirred chamber", *IEEE Transactions on Electromagnetic Compatibility*, Vol. 33, No. 4, pp 366-370, Nov. 1991.

[15] D. A. Hill, M. T. Ma, A. R. Ondrejka, B. F. Riddle, M. L. Crawford, and R. T. Johnk, "Aperture excitation of electrically large, lossy cavities", *IEEE Transactions on EMC*, vol. 36, no. 3, pp. 169–178, Aug. 1994.

[16] M. Bäckström, O. Lundén, P-S. Kildal, "Reverberation chambers for EMC susceptibility and emission analyses", *Review of Radio Science* 1999-2002, pp. 429-452.

[17] K. Rosengren, P-S. Kildal, C. Carlsson, J. Carlsson, "Characterization of Antennas for Mobile and Wireless Terminals in Reverberation Chambers: Improved Accuracy by Platform Stirring", *Microwave and Optical Technology Letters*, Vol. 30, No 20, pp 391-397, Sept 2001

[18] P-S. Kildal, C. Carlsson, "Detection of a polarization imbalance in reverberation chambers and how to remove it by polarization stirring when measuring antenna efficiencies", *Microwave and Optical Technology Letters*, Vol. 32, No 2, pp. 145-149, July 20, 2002

[19] A. Wolfgang, J. Carlsson, C. Orlenius and P-S. Kildal, "Improved procedure for measuring efficiency of small antennas in reverberation chambers", *IEEE AP-S International Symposium*, Columbus, Ohio, June 2003.

[20] P-S. Kildal and C. Carlsson, *TCP of 20 Mobile Phones Measured in Reverberation Chamber - Procedure, Results, Uncertainty and Validation*, Bluetest AB report, Feb 2002.

[21] P-S. Kildal, C. Carlsson, "Comparison between head losses of 20 phones with external and built-in antennas measured in reverberation chamber", *IEEE AP-S International Symposium*, San Antonio, Texas, June 2002.

The information contained in this document should be used only for the scope of the contract for which this document is prepared.

[22] www.tcodevelopment.com

[23] A. Wolfgang, C. Orlenius and P-S. Kildal, "Measuring output power of Bluetooth devices in a reverberation chamber", *IEEE AP-S International Symposium*, Columbus, Ohio, June 2003.

[24] P-S. Kildal, K. Rosengren, J. Byun, J. Lee, "Definition of effective diversity gain and how to measure it in a reverberation chamber", *Microwave and Optical Technology Letters*, Vol. 34, No 1, pp. 56-59, July 5, 2002.

[25] P-S. Kildal, K. Rosengren, "Electromagnetic analysis of effective and apparent diversity gain of two parallel dipoles", *IEEE Antennas and Wireless Propagation Letters*, Vol. 2, No. 1, pp 9-13, 2003

[26] P.-S. Kildal and K. Rosengren, "Correlation and capacity of MIMO systems and mutual coupling, radiation efficiency and diversity gain of their antennas: Simulations and measurements in reverberation chamber", *IEEE Communications Magazine*, vol. 42, no. 12, pp. 102-112, Dec. 2004.

[27] K. Rosengren and P.-S. Kildal, "Radiation efficiency, correlation, diversity gain, and capacity of a six monopole antenna array for a MIMO system: Theory, simulation and measurement in reverberation chamber", *Proceedings IEE, Microwaves, Optics and Antennas*, Feb. 2005.

[28] R. Bourhis, C. Orlenius, G. Nilsson, S. Jinstrand and P.-S. Kildal, "Measurements of realized diversity gain of active DECT phones and base-stations in a reverberation chamber", *IEEE AP-S International Symposium*, Monterey, California, June 2004.

[29] H. A. Wheeler, "The radiansphere around a small antena", *Proceedings of IRE*, pp. 1325-1331, Aug. 1959

[30] K.P. van der Riet, B.A. Austin, „Limitations of the Wheeler method for measuring antenna radiation efficiency due to cavity resonant modes, *The Transactions of the SA Institute of Electrical Engineers*, December 1987

[31] R.H. Johnston, J. G. McRory, "An Improved Small Antenna Radiation-Efficiency Measurement Method", *IEEE AP-Magazine*, Vol.40, No.5, October 1998

[32] Geissler, M., Litschke, O., Heberling, D., Waldow, P. and Wolff, I., 'An improved method for measuring the radiation efficiency of mobile devices', *IEEE Antennas and Propagat. Society. Symp*, 2003.

[33] M. Geissler, O. Litschke, A. Winkelmann, D. Heberling, P. Waldow, "Accurate Measurement characterisation of mobile terminal antennas", *International ITG Conference on Antennas*, Berlin (Germany), September 2003.

The information contained in this document should be used only for the scope of the contract for which this document is prepared.

[34] E.H. Newman, P. Bohley, C.H. Walter, „Two Methods for the Measurement of Antenna Efficiency“, *IEEE Trans On Ant. And Propagation*, Vol.AP-23, No. 4, S.457-461, July 1975.

[35] R. F. Harrington, "Effect of antenna size on gain, bandwidth and efficiency", *Journal or Research of the National Bureau of Standards – D. Radio Propagation*, vol. 64D, No. 1, January-February 1960, pp. 1-12

[36] O. Staub, J-F. Zürcher, A. Skrivervik, "Some considerations on the correct measurement of the gain and bandwidth of electrically small antennas", *Microwave and Optical Technology Letters*, vol. 17, no. 3, February 1998, pp. 156-160.

The information contained in this document should be used only for the scope of the contract for which this document is prepared.